Quim. Nova, Vol. 42, No. 4, 447-452, 2019 http://dx.doi.org/10.21577/0100-4042.20170353

Nota Técnica

DEVELOPMENT OF AN AUTOMATED METHOD TO PERFORM A QUANTITATIVE STUDY OF PARTICLE SIZE DISTRIBUTION AND THE EFFECT OF A CONDUCTIVE LAYER IN SCANNING ELECTRON MICROSCOPY

Juan C. G. Barreto[a], Diego L. Tita[a] and Marcelo O. Orlandi[a,*]
[a]Instituto de Química, Universidade Estadual de São Paulo, 14800-060 Araraquara – SP, Brasil

Recebido em 23/01/2019; aceito em 13/03/2019; publicado na web em 08/04/2019

The determination of particle size distribution is an important parameter for controlling industrial processes, particularly in the field of pharmaceuticals. It is also an important parameter for characterizing nanoparticles. The best technique for determining particle size distribution is scanning electron microscopy. The process of counting particles is typically performed manually, which requires both more time and a higher standard deviation than automatic methods. This study shows the results of a particle counting procedure that relies on a fully automated method that was found to improve the reproducibility of the measurement. The effect on the diameter of near-spherical polymer nanospheres between 20 and 100 nm (mean of 60 nm) when samples were coated by a conducting layer (such as gold or carbon) was also evaluated. The images were collected using a field emission scanning electron microscope and then processed using the ImageJ program. Results showed that the method proposed in this work produces mean diameter values in accordance with NIST-traceable near-spherical polymer nanospheres for the sample without coating. The study also revealed two main effects of the conductive coating: changes to topography and an increase in mean particle diameter.

Keywords: particle size distribution; near-spherical polymer nanoparticles; gold coating; carbon deposition; scanning electron microscopy.

INTRODUCTION

Particle size distribution (PSD) and surface morphological characteristics are the most important analyses when studying nanoparticles, and the scanning electron microscope is very useful for these tasks.[1] Non-conductive or poorly conducting materials such as pharmaceuticals, some ceramics, polymers, glass, and organic materials may need surface treatment before they can be analyzed under optimal conditions by an electron microscope. A conductive layer is usually necessary to reduce the effect of the electric charge on the surface caused by the interaction between the electron beam and the sample, which can result in image distortion. In addition, the primary beam also may cause thermal and radiation damage, thus leading to the deterioration of the sample.[2]

In some extreme cases, the sample may acquire sufficient charge on surface to significantly decelerate the primary beam. According to Goldstein *et al.*,[2] two main procedures can be used to avoid or minimize the effect of surface charge: (i) modification of the specimen by increasing its surface conductivity through a coating with a thin layer of a conductive material (e.g. carbon or metal coating such as silver, gold, platinum, chromium, aluminum, or gold-palladium alloys), and (ii) modification of the environment in which the specimen is being studied (i.e. increasing its conductivity by infusing it with conducting compounds or performing the analysis in an environmental scanning electron microscope for samples that exhibit humidity and/or are uncoated). In the latter case, however, the improvement to the charge effect on the surface is accompanied by a worsened resolution.

The sample's conductive layer is usually deposited using either thermal evaporation or sputter coating. A carbon wire or belt is an important material used in thermal evaporation: when heated to its vaporization temperature using a high electric current in a vacuum, it evaporates rapidly into a monoatomic state. For direct current (dc) sputtering, coating metals (Au) or alloys (Au-Pd, Pt-Pd) are used as a target.[2]

*e-mail: marcelo.orlandi@unesp.br

One of the most important steps for characterizing materials using electron microscopy is acquiring images that are interpretable and which provide accurate information about the sample under study.[3] A good image must exhibit good levels of brightness and contrast and must provide a sufficient number of particles with a good resolution. It must also have an acceptable number of image pixels such that any uncertainties associated with the measurements are minimized during image processing.[3]

Image processing approaches can be classified as a manual, software-assisted, or automated. The manual process consists of a direct measurement using a ruler and a calibrated photomicrograph. The software-assisted method employs image analysis packages, such as ImageJ software, which use a line measurement tool to determine the diameters of particles. Both the manual and software-assisted methods produce errors due to sample size limitations and require tedious and repeated measurements.[3]

The automated methods, which rely on automated software packages, have several thresholding algorithms designed to locate and measure particles. In addition to the mean and median particle diameter values, the automated methods can provide other important information, including perimeter, area, roundness, and mode.[4] In addition, some programs include tools to calculate and plot the histogram for a particle sample or population. However, the disadvantage of the automated method for counting particles lies in the errors introduced into the analysis through the loss of information and the induction of artifacts during image processing.[3] Each algorithm has different criteria for discriminating particle edges from the background, and these algorithms can produce significantly different results.

All of these factors influence the particle diameter measurement, especially when the sample is coated. Thus, the main objective of this study was to develop a user-friendly and automated method dependent upon open-access software to determine the particle size distribution of a microscopy image. Additionally, we studied the influence of carbon and gold deposition on the morphological characteristics of near-spherical polymer nanoparticles.

EXPERIMENTAL METHODS

Sample Preparation

NIST-traceable polymer nanospheres (Cat No 3060A) with particle diameters of 60 ± 2.7 nm were used in this study. Samples were prepared in an aqueous solution (0.0125% m/v) and dispersed using an ultrasonic bath (Ultrasonic Cleaner, model 1440D) for 3 min. Then, one drop of suspension was deposited on a conductive silicon substrate and dried for 48 hours in a desiccator containing silica spheres desiccant in a vacuum medium at room temperature. All of the samples were prepared in triplicate.

Polymer is a known non-conductive material. We therefore prepared a control sample with no coating; we also studied the morphological characteristics of polymer spheres coated with a carbon or gold layer to avoid effects of a surface charge. Table 1 shows a detailed description of the samples' coating conditions and their labels. All of the parameters were chosen according to the criteria used to meet SEM sample preparation conditions in the Advanced Microscopy Laboratory (LMA) of the Chemistry Institute of São Paulo State University (UNESP) in Araraquara, São Paulo, Brazil.

A BAL-TEC coating system (model SCD-50) equipped with a turbomolecular vacuum pump (EDWARDS T-STATION/75DX-NW40) was used for the coatings. The distance between the target and the sample was kept at 50 mm for all depositions. During deposition, the vacuum was kept at $2x10^{-1}$ mbar.

Image Acquisition

All of the images were collected using a cold field emission scanning electron microscope (FE-SEM; JEOL model 7500F) with the following operating conditions: accelerating voltage of 2 kV, emission current of 10 uA, current probe of 9, work distance at 7.7 mm, secondary electron image (SE) mode, and 100,000x magnification (1 pixel = 0.935 nm). It is worth to mention the importance of selecting the correct degree of magnification. Acquiring images at higher magnification will require more images to count the minimum number of particles, thus requiring more time for the processing step. On the other hand, smaller magnification can produce an image that includes more particles but increases the particle size error due to the poor resolution. The magnification provided by different microscopes can vary even if they present the same scale, so a practical tip is to collect images in which each particle has a minimum of 100 square pixels.

Image Processing

The particle size distribution of the near-spherical polymer nanoparticles was obtained using the automated method. This method consists of a threshold algorithm to locate and measure the particles.[3] More than fifty FE-SEM images were acquired for each sample and, on average, five particles were counted per image. During the image processing step, the particles that were close to the edges of the image were not considered in order to avoid the stretching effect of shapes. In addition, we performed tests as part of all counts in order to consider the effect of particle boundaries. Uncertainness was also determined by considering both the effect of edges and NIST traceability errors, which are the main sources of uncertainly.

During the particle counting procedure, a threshold must be applied to distinguish the particles from the substrate. The threshold algorithm selected was the intermodes algorithm[5] due to its superior performance relative to the other algorithms tested. Particle diameters were obtained using the area of particles and the assumption that they were spherical, which is a good approximation in the present study. Particle area was limited to values between 314 nm^2 (359 $pixels^2$) and 7854 nm^2 (8984 $pixels^2$); as a result, the minimum and maximum particle diameters were 20 and 100 nm, respectively. These limit values were obtained using the formula for the area of a circle and the pixel size of the images.

The images were processed using the ImageJ software, version 1.49, which is a powerful license-free tool for image treatment (for more details, see the supplementary material). It is important to note that all of the aforementioned steps can be applied using other similar software, so the method reported herein exhibits general validity. To generate the histogram showing particle size distribution, approximately 250 particles had to be counted. The histogram data were fit using the SciDAVis software, version 1.D013, which is also a license-free program.

RESULTS AND DISCUSSION

Electron microscopy images can be represented by a histogram, which is a plot of the number of pixels (*y* axis) with their respectively grayscale value (*x* axis). For example, supposing an 8 bit image, the abscissa displays the 256 levels of gray and the coordinate axis represents the levels of intensity (counts) of the image. Each peak in the histogram should correspond to one kind of structure in the image so it can be used to distinguish between the particles and the substrate. Several algorithms can be employed to locate, identify, and measure the particles on the substrate using the brightness histogram as part of the thresholding process. In this study, the intermodes algorithm developed by Prewitt and Mendelsohn was applied;[5] it is based on images in which the object and the background pixels are separable. According to Fazeli *et al.*[6] and Namgung *et al.*[7], the extracted features correspond to the location of the peaks. Figure 1A shows a typical FE-SEM image of the polymer nanoparticles from the control sample, while Figure 1B presents two peaks in the histogram, the first of which represents the background (lower grayscale values), and the second of which represents the particles (higher grayscale values). In the intermodes algorithm,[5] the threshold value is the mathematical mean between the first and second peaks of the histogram. Thus, this grayscale value is considered the limit between the particle and the substrate.

Figure 2 illustrates a typical example of image processing for the control sample. Using the original image (Figure 2A), the brightness

Table 1. Experimental conditions for coating near-spherical polymer nanoparticles

Sample	Element Deposition	Deposition time (s)	Carbon Thread	Mode	Current (mA)
Control	-	-	-	-	-
Au_20s	Gold	20	-	Sputtering	40
Au_50s	Gold	50	-	Sputtering	40
C_1	Carbon	-	1 flash	Evaporation	-
C_2	Carbon	-	2 flash	Evaporation	-

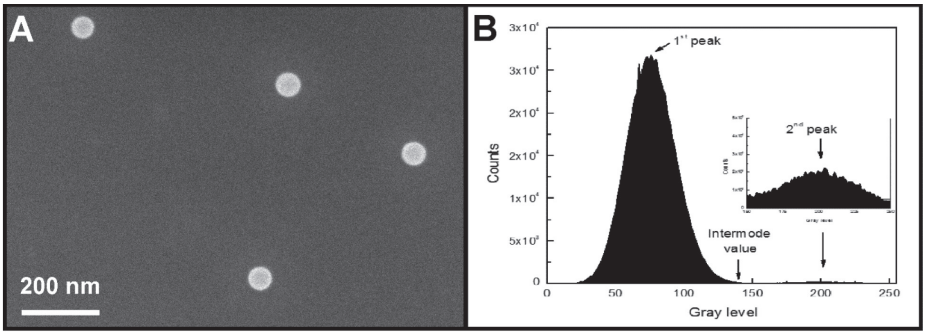

Figure 1. *(A) FE-SEM image of the control sample and (B) the respectively gray scale level histogram. The arrows indicate the peak position of higher and lower gray values used at the intermodes algorithm*

and the contrast were enhanced to produce Figure 2B. Figure 2C is the result after the application of the intermodes algorithm threshold. The comparison of Figures 2A and 2C clearly shows that the intermodes threshold produces a binary image in which the polymer particles are represented. Figure 2D shows the outlines of particles.

In some images in which the objects of interest did not share a single brightness or color value, such as Figure 3A, the threshold was applied to the background (the substrate) (Figure 3B), since the grayscale values that corresponded to the substrate on the histogram were more uniform than those of the objects. The resulting binary image (Figure 3B) was then inverted to produce the representation of the particles (Figure 3C). In images like Figure 3D, the binary algorithm (watershed segmentation) can be used to separate the particles, as described by Beucher[8] and Sun *et al.*[9] (Figure 3E). This option, however, is not recommended because the borders of each particle become unclear. The best decision is to erase agglomerated particles (bottom right in Figure 3F) or to select another image that has no agglomerated particles. Figure 3 exemplifies the image processing steps performed to identify and isolate particles using the above-mentioned tools. It is important to note that acquiring a good image during SEM analysis allows for a significant reduction in the time required for the image processing step.

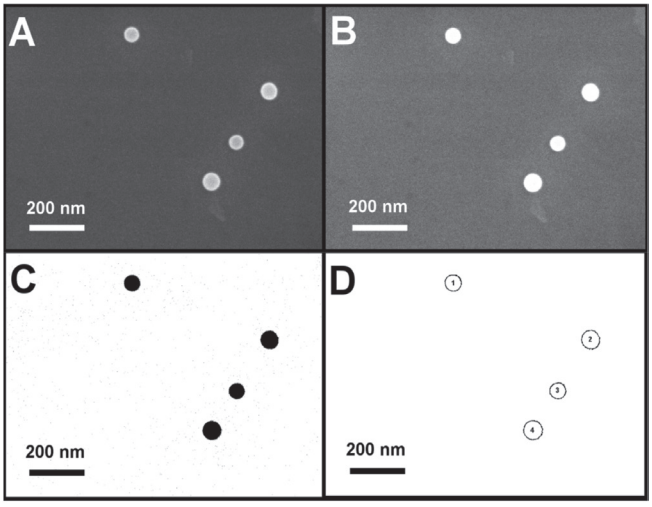

Figure 2. *Example of image processing at the control sample. A) Original FE-SEM image, B) Image after brightness and contrast adjust, C) Image after the threshold process, and D) Outlines of nanoparticles*

Particle area was determined using the Analyze Particle tool within the ImageJ software. This command processes the threshold binary image by identifying the particles and calculating their areas. The software reports the results individually in a table. Assuming that the particles were spherical, the diameters were calculated using Equation 1:

$$d = 2\sqrt{\frac{A}{\pi}} \quad (1)$$

where A is the calculated area and d is the diameter of the particle. For particles that are not spherical, Equation 1 can still be used and will provide the equivalent spherical diameter of particles.

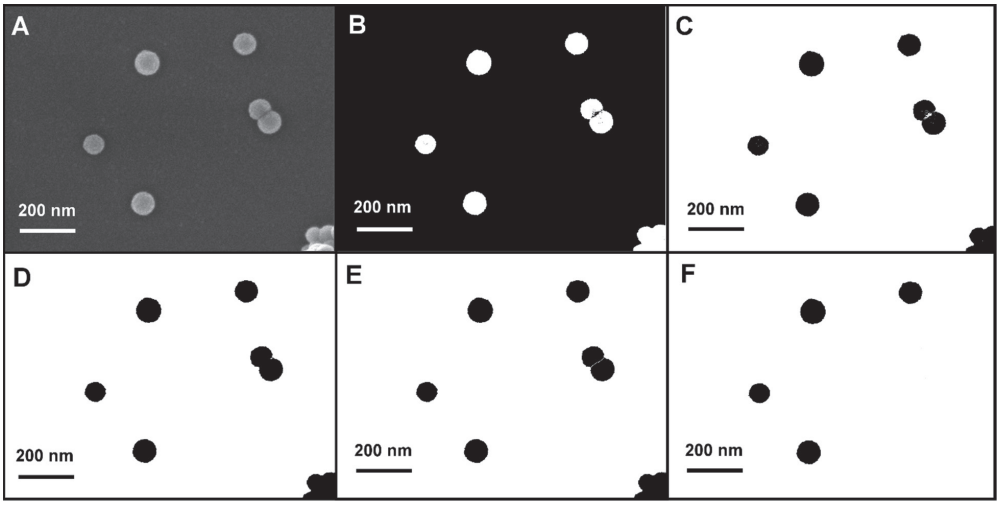

Figure 3. *Sequence of the image processing on sample coated twice with carbon fiber. A) Original image, B) Image obtained after applying the binary threshold, C) Image with the binary threshold inversion, D) Image after applying fill holes process, E) Image after particle separation process (Watersheld) and F) Image after the discrimination of nanoparticles*

The particle size distribution was exhibited on a histogram (Figure 4B), and the data were fit with the log-normal distribution (Equation 2[10]) to determine the mean and standard deviation (SD) of the sample (Figure 4B).

$$f(x) = \frac{1}{x\sqrt{2\pi}\ ln\ S_g} \exp\left[-\frac{(ln\,x - ln\,x_g)^2}{2\ ln^2 S_g} \right] \quad (2)$$

where X_g is the geometric mean diameter and S_g is the geometric SD.

Figure 5 shows a representative image of each sample studied herein with the conducting layer. Figures 5A and 5B present the typical gold deposition structure, producing nano-islands on the substrates. This phenomenon can be attributed to the high density of gold, which is responsible for producing large grain size during the sputtering process.[11] Figures 5C and 5D show the effect of the number of carbon depositions on the substrate. Though the diameter of the particles appears to increase, the particles surface is less smooth when two depositions are used. Although the deposition of a conductive layer over non-conducting samples is important in

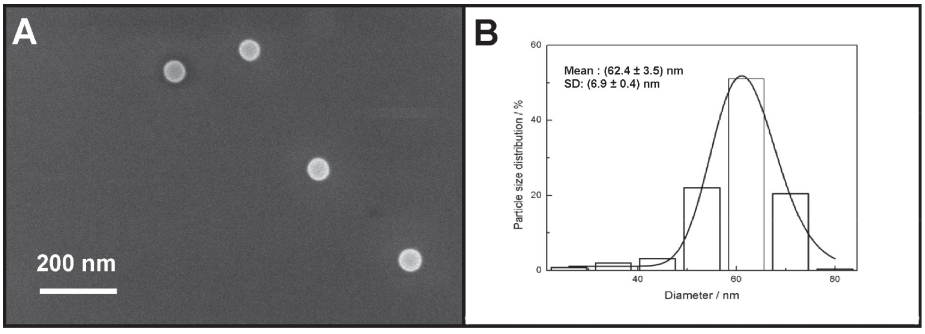

Figure 4. *(A) FE-SEM image of near-spherical polymer nanoparticles without coating and (B) the respective histogram of particle size distribution*

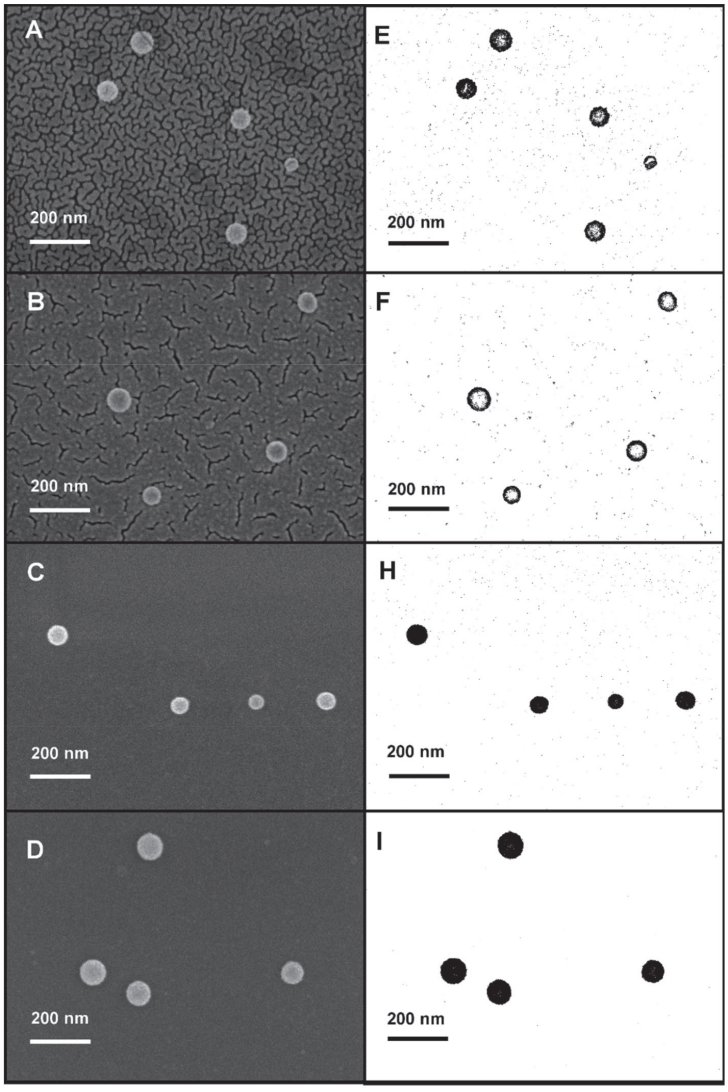

Figure 5. *FE-SEM image of near-spherical polymer nanoparticles: A-B) coated with gold, 20 s and 50 s, respectively, C-D) After carbon deposition using 1 and 2 fibers, respectively. On the right column (E-I) is shown the result of applying the binary threshold process at images from the left column*

order to avoid effects of charges, the layer clearly alters the shape and the surface roughness of particles. Figure 5 also shows that gold deposition produces more roughness in particles surface than the carbon deposition, which seems to be more homogeneous over the surfaces of the samples. A thinner layer of gold suggests a greater level of roughness, and this correlation is evident on substrate surfaces seen in the images produced by the SEM (Figure 5A). In addition, when the deposited layer becomes thicker, the level of roughness decreases (Figure 5B); however, the shape of the particles changes and their diameters increase. In general, both gold and carbon deposition alter the surface characteristics.

Nevertheless, during the image acquisition process, samples without coating exhibited horizontal lines characteristic of surface charging. Moreover, the particles were burned after long periods of exposure to the electron beam. It is important to note that both effects can be minimized when modern microscopes are used by applying a potential at the sample substrate, thus producing a decelerated electron beam.

In contrast, the effect of charges during image acquisition disappeared in both the gold-and the carbon-coated samples. Surface burning was also minimized or eliminated. In a real-world application, it is not possible to control all of the parameters required to obtain an ideal SEM image. Though the thin layer of gold deposited onto the substrate improves image acquisition and increases electron scattering and brightness levels, it significantly alters the shape and the surface roughness of particles. These changes jeopardize image processing during the mask step, thus making it more difficult for a good threshold to be obtained. The gold islands negatively influenced the levels of histogram producing holes inside the particles (Figure 5E and 5F). The surface changes of the carbon-coated samples were less significant than those of the samples on which gold was deposited, and these images enabled a good threshold step during image processing (Figure 5H and 5I).

The results show that the intermodes algorithm produced a good threshold for separating particles from the substrate in SEM images. Moreover, the results suggest that the same method could be applied to images acquired via transmission electron microscopy (TEM), atomic force microscopy (AFM), and optical microscopy (OM), since microscope is calibrated and the characteristic and peculiarities of each technique was considered.

Figure 6 shows the results of the particle size distribution in the samples after coating with gold (Figure 6A and 6B) and carbon (Figure 6C and 6D) obtained using the automated method. Table 2 summarizes the average diameter for all of the samples in this study. The mean and SD values of the control sample (62.4 ± 3.5 nm and 6.9 ± 0.4 nm, respectively) were in agreement with the NIST certificate. Both Table 2 and Figure 6 show that the mean diameter of the particles was higher in the coated samples (gold or carbon). The particle size distribution results suggest that one and two carbon layer deposits increased the diameter of particles by approximately 11.4 nm and 20.6 nm, respectively, which is more than 30% increase in the latter case. The gold deposition increased the particle diameter by 4.3 nm (6.9%) after 20 s of deposition and by 12.7 nm (20.3%) after 50 s of sputtering time. The thinnest layer of gold deposition

Table 2. Means and standard deviations values of sample with a different conditions of coating and its uncertainty

Sample Name	Average size (nm)	St. Dev. (nm)
Control	62.4 ± 3.5	6.9 ± 0.4
Au_20	66.7 ± 3.7	4.6 ± 0.3
Au_50	75.1 ± 4.2	6.8 ± 0.4
C_1	73.8 ± 4.1	8.1 ± 0.4
C_2	83.0 ± 4.6	5.8 ± 0.3

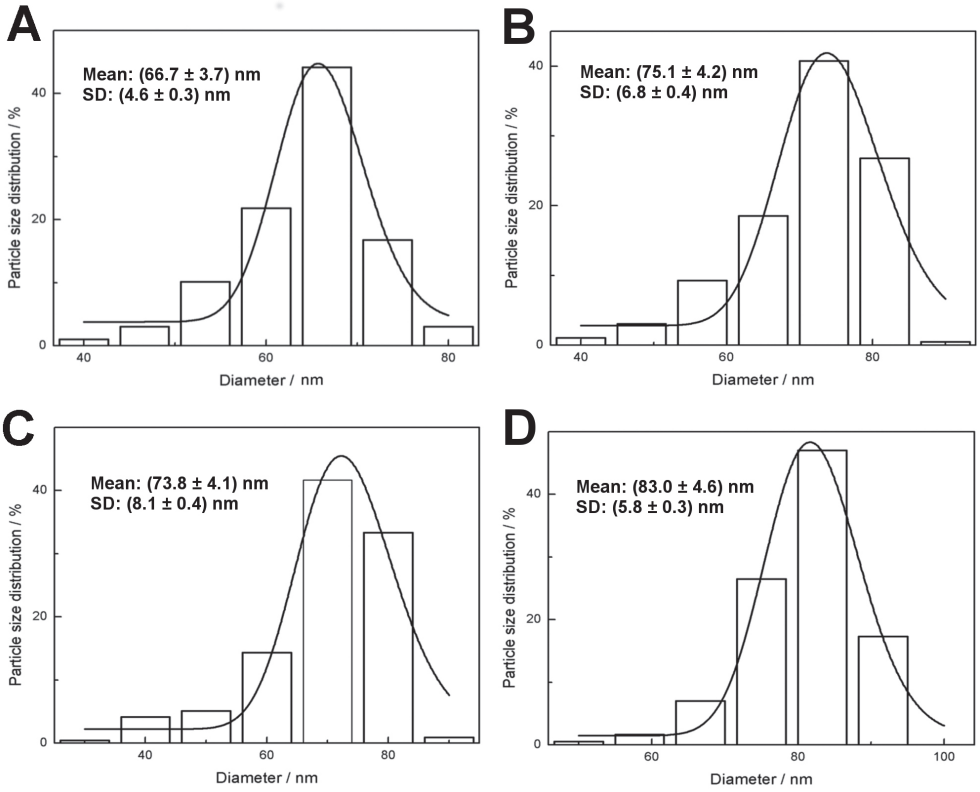

Figure 6. *Histogram of particle size distribution and the fit curve related to the system: A) Au_20, B) Au_50, C) C_1 and D) C_2*

was associated with both the highest gold density and the smallest amount of material deposited on the surface of the sample.

Finally, the results were successful for determining particles of approximately 60 nm in diameter, but these results can be applied broadly since microscope scale is calibrated. Based on our experience, particles up to 100 μm in diameter can be measured using this method. The image processing method shown herein is simple, easy, and accurate, and can facilitate the creation of a histogram showing the particle size distribution of the sample. Moreover, the method proposed herein eliminates operator influence, thus producing consistent results when the steps are followed correctly.

CONCLUSION

The use of an automated method for determining particle size distribution was successful. The mean particle size values determined by electron microscopy agrees with the mean values for NIST-traceable polymer nanospheres, a result which reflects the validity of this method. Gold and carbon coatings were found to influence the shape and surface roughness of polymer nanoparticles. The coating process was found to minimize the effect of electric charges and to enhance brightness and contrast, but the process produces changes to particle size, shape, and surface texture. In this study, the thin layers of gold (deposited by sputtering) and of carbon (deposited by thermal evaporation) on near-spherical nanoparticles increased the diameter of the particles from 4.3 nm to 20.6 nm, depending on the deposition process. Gold deposition can produce thinner layers and significantly affect the particles' characteristics, generating gold islands on the surface. On the other hand, carbon deposition can produce a larger final average particle diameter than gold deposition can; it also produces a thick carbon coating that can alter the fine details on the particle's surface. Based on these results, it is recommended that non-conductive materials, such as pharmaceuticals, ceramics, and polymers, be tested to observe particles without surface coating using techniques provided by modern microscopes, such as gentle beam mode. When necessary, the deposition material chosen must be related to the sample analysis desired: if studying surface details is the main objective of the analysis, a carbon layer can be used, but if the average particle size is the most important parameter of analysis, the gold layer will have less of an influence.

SUPPLEMENTARY MATERIAL

The tutorial of the process for obtaining the particle size distribution using imageJ software is available free of charge at http://quimicanova.sbq.org.br, in pdf format.

ACKNOWLEDGMENTS

The authors would like to thank the CNPq, Brazilian research agency, [402297/2013-0, 303542/2015-2 and 443138/2016-8] for the financial support. Prof. M. Jafellicci Jr is thankful for supplying the near-spherical polymer nanoparticles sample. We also thanks the LMA-IQ-UNESP laboratory for providing SEM facilities.

REFERENCES

1. Ranjit, K.; Baquee, A. A.; *Int. Res. J. Pharm.* **2013**, *4*, 47.
2. Goldstein, J.; Newbury, D. E.; Echil, P.; Joy, D. C.; Romig Jr., A. D.; Lyman, C. E.; Fiori, C.; Lifshin, E.; *Scanning electron microscopy and X-ray microanalysis*; 2nd ed., Springer: New York, 1992.
3. Pyrz, W. D.; Buttrey, D. J.; *Langmuir* **2008**, *24*, 11350.
4. Russ, J. C.; *The image processing handbook*, 4th ed., CRC Press LLC: Boca Raton, 1999.
5. Prewitt, J. M. S; Mendelsohn, M. L.; *Ann. N. Y. Acad. Sci.* **1996**, *128*, 1035.
6. Fazeli, F.; Sarrafzadeh, A.; Shanbehzadeh, J.; *Proceedings of the International MultiConference of Engineers and Computer Scientists* **2013**, *1*, 13.
7. Namgung, B.; Ong, P. K.; Wong, Y. H.; Lim, D.; Chun, K. J.; Kim, S.; *Physiological Measurement* **2010**, *31*, 61.
8. Beucher, S.; *Scanning Microsc.* **2000**, *6*, 26.
9. Sun, H. Q.; Luo, Y. J.; *J. Microsc. (Oxford, U. K.)* **2009**, *233*, 326.
10. Endo, Y.; *Powder Technol.* **2009**, *193*, 154.
11. Echlin, P.; *Handbook of sample preparation for scanning electron microscopy and X-ray microanalysis*, Springer: New York, 2009.